Received: 31 March 2017 | Revised: 29 January 2018 | Accepted: 30 January 2018

DOI: 10.1002/hbm.23997

RESEARCH ARTICLE

WILEY

# Oscillatory dynamics in the dorsal and ventral attention networks during the reorienting of attention

Amy L. Proskovec[1,2] | Elizabeth Heinrichs-Graham[2,3] | Alex I. Wiesman[2,3] | Timothy J. McDermott[2] | Tony W. Wilson[1,2,3]

[1]Department of Psychology, University of Nebraska - Omaha, Omaha, Nebraska

[2]Center for Magnetoencephalography, University of Nebraska Medical Center (UNMC), Omaha, Nebraska

[3]Department of Neurological Sciences, UNMC, Omaha, Nebraska

**Correspondence**
Tony W. Wilson, PhD, Center for Magnetoencephalography, University of Nebraska Medical Center, 988422 Nebraska Medical Center, Omaha, NE 68198, USA.
Email: twwilson@unmc.edu

**Funding information**
National Institute of Mental Health, Grant/Award Number: R01 MH103220; National Science Foundation, Grant/Award Number: 1539067; Nebraska Health System; University of Nebraska Medical Center

## Abstract

The ability to reorient attention within the visual field is central to daily functioning, and numerous fMRI studies have shown that the dorsal and ventral attention networks (DAN, VAN) are critical to such processes. However, despite the instantaneous nature of attentional shifts, the dynamics of oscillatory activity serving attentional reorientation remain poorly characterized. In this study, we utilized magnetoencephalography (MEG) and a Posner task to probe the dynamics of attentional reorienting in 29 healthy adults. MEG data were transformed into the time-frequency domain and significant oscillatory responses were imaged using a beamformer. Voxel time series were then extracted from peak voxels in the functional beamformer images. These time series were used to quantify the dynamics of attentional reorienting, and to compute dynamic functional connectivity. Our results indicated strong increases in theta and decreases in alpha and beta activity across many nodes in the DAN and VAN. Interestingly, theta responses were generally stronger during trials that required attentional reorienting relative to those that did not, while alpha and beta oscillations were more dynamic, with many regions exhibiting significantly stronger responses during non-reorienting trials initially, and the opposite pattern during later processing. Finally, stronger functional connectivity was found following target presentation (575-700 ms) between bilateral superior parietal lobules during attentional reorienting. In sum, these data show that visual attention is served by multiple cortical regions within the DAN and VAN, and that attentional reorienting processes are often associated with spectrally-specific oscillations that have largely distinct spatiotemporal dynamics.

**KEYWORDS**
dorsal attention network, functional connectivity, magnetoencephalography, oscillation, Posner cueing task, ventral attention network

## 1 | INTRODUCTION

The ability to orient attention to behaviorally relevant sensory information and stimuli is central to the successful execution of higher level cognitive operations. Equally important is the ability to shift the focus of attention to new incoming information, an operation commonly referred to as attentional reorientation. Perhaps the most widely utilized task for assessing the orientation and reorientation of attention has been the Posner cueing task (Posner, 1980). Briefly, the task consists of a cue that precedes the presentation of a target stimulus. The cue serves as a temporal alerting mechanism for the impending target, and additionally can provide spatial information about the upcoming target. The cue can be either valid, such that it resides in the same location as the target, or invalid, such that it resides in a location different than the target. When the cue is invalid, attention must be reoriented to the location of the target stimulus (Corbetta, Patel, & Shulman, 2008). Typically, participants respond more slowly to invalid relative to valid targets. This phenomenon is known as the validity effect (Vossel, Thiel, & Fink, 2006).

Many studies have examined the brain regions serving the orienting and reorienting of attention, and these regions are commonly segregated into two networks: the dorsal attention network (DAN) and the ventral attention network (VAN; Corbetta et al., 2008; Petersen & Posner, 2012). The DAN includes the bilateral superior parietal lobules,

  

intraparietal sulci, and frontal eye fields, and is thought to be involved in top–down control processes and the cognitive selection of information that is relevant to current goals (Corbetta et al., 2008). Activation of the DAN has also been linked to expectations about forthcoming sensory information, as well as the associated motor responses for goal-driven attention (Corbetta et al., 2008). In agreement with these findings, activation of the DAN has been consistently reported during both the cue and target intervals of the Posner task (Shulman & Corbetta, 2012).

In contrast, the VAN is thought to be integral to the detection of behaviorally relevant stimuli (Corbetta et al., 2008; Petersen & Posner, 2012). Thus, it is often selectively activated during target presentation in the Posner task, particularly during the detection and processing of invalid targets (Corbetta et al., 2008). The nodes of the VAN are predominantly right-lateralized and include the temporoparietal junction and ventral frontal cortex (Corbetta et al., 2008). Of note, stronger activation within both the DAN and VAN has also been demonstrated during the reorienting of attention (Corbetta et al., 2008; Vossel, Geng, & Fink, 2014). For example, using fMRI and the Posner task, Vossel, Weidner, Thiel, and Fink (2009) compared invalid versus valid trials and found increased neural activity in both the DAN (i.e., right superior parietal lobule) and VAN (i.e., bilateral temporoparietal junction). Other fMRI studies have reported similar results (Doricchi, Macci, Silvetti, & Macaluso, 2010; Indovina & Macaluso, 2007; Leitao, Thielscher, Tunnerhoff, & Noppeney, 2015; Macaluso & Patria, 2007; Thiel, Zilles, & Fink, 2004; Xuan et al., 2016). Thus, while both attention networks are distinct, they are also closely intertwined during the reorienting of attention (Vossel et al., 2014).

While the brain regions serving the orienting and reorienting of attention have been well characterized via fMRI investigations, less is understood about the dynamics of oscillatory activity that underlie attentional reorienting. In general, previous studies examining neural oscillations in this context have focused on attentional orienting during the cue period (i.e., not attentional reorienting). Such studies have broadly shown decreased activity in lower frequency bands (i.e., $< 30$ Hz) across frontal, parietal, and occipital regions, as well as increased gamma band (i.e., $> 30$ Hz) activity in visual cortex (Deiber, Ibanez, Missonnier, Rodriguez, & Giannakopoulos, 2013; Fan, McCandliss, Fossella, Flombaum, & Posner, 2007; Rihs, Michel, & Thut, 2009; Siegel, Donner, Oostenveld, Fries, & Engel, 2008). Although these studies have provided critical insight on the dynamics of oscillatory activity serving the orienting of attention, they did not assess the reorienting of attention to invalid targets. In fact, only a handful of previous neurophysiological studies have examined attentional reorienting by assessing validity effects following target presentation. One study reported greater global field power during invalid relative to valid trials following target presentation (Nagata, Bayless, Mills, & Taylor, 2012), while two other studies found stronger event-related potentials in posterior electrodes during the processing of valid compared to invalid trials (Busch & VanRullen, 2010; Cosmelli et al., 2011). A fourth study reported decreased alpha activity in posterior electrodes contralateral to the target hemifield in both valid and invalid conditions, but that this response was significantly delayed following invalid target presentation (Sauseng et al., 2005). However, of these four studies, three did not utilize any form of time–frequency or spectral analysis methods when assessing attentional reorientation, and the only study that did use such methods did not attempt to image or localize the neural origin of oscillatory differences. Moreover, the main findings of the studies were not consistent. Thus, the dynamics of oscillatory activity underlying the reorienting of attention remain largely uncharacterized.

The purpose of this study was to address this specific gap in the literature. Briefly, using spatially resolved magnetoencephalography (MEG), we investigated the neural oscillatory activity and functional connectivity serving attentional reorienting in healthy adults. We broadly hypothesized that neural oscillations would be observed during both valid and invalid targets within regions of the DAN and VAN, and that distinct patterns of oscillatory activity would emerge between specific frequency bands. As decreased alpha and/or beta activity is thought to reflect the active engagement of the region during task performance (Klimesch, 2012; Klimesch, Sauseng, & Hanslmayr, 2007), we expected reduced alpha and beta activity within attention networks during target presentation, irrespective of cue validity. However, we also thought that these oscillatory responses would be uniquely modulated by cue validity. Essentially, greater decreases in alpha and beta activity were anticipated during early processing of valid relative to invalid targets, while the opposite effect was expected later during target processing. This pattern was hypothesized because valid targets should be processed more rapidly relative to invalid targets, and we believe that alpha and beta activity primarily reflect target processing rather than attentional reorienting. In contrast, we hypothesized that theta activity within attention networks would increase during target presentation, and that these increases would be stronger during invalid targets relative to valid targets. This hypothesis was based on previous transcranial magnetic stimulation data suggesting that attention reorients periodically at the theta frequency (Dugue, Roberts, & Carrasco, 2016), and an electrocorticography (ECoG) study in patients with epilepsy that also linked theta and the reorienting of attention (Daitch et al., 2013). Finally, we also hypothesized that functional connectivity between nodes of the DAN and VAN would be increased during target presentation, as previous studies have reported increased functional connectivity during visuospatial attention tasks (Sauseng et al., 2005; Siegel et al., 2008).

## 2 | METHODS AND MATERIALS

### 2.1 | Subject selection

We studied 29 healthy adults (12 females; mean age: 31.83, *SD*: 6.93, range: 22–45) who were recruited from the local community. Exclusionary criteria included any medical illness affecting CNS function, neurological disorder, history of head trauma, current substance abuse, and the MEG Laboratory's standard exclusion criteria (e.g., dental braces, metal implants, and/or any type of ferromagnetic implanted material). After a complete description of the study, written informed consent was obtained from participants following the guidelines of the

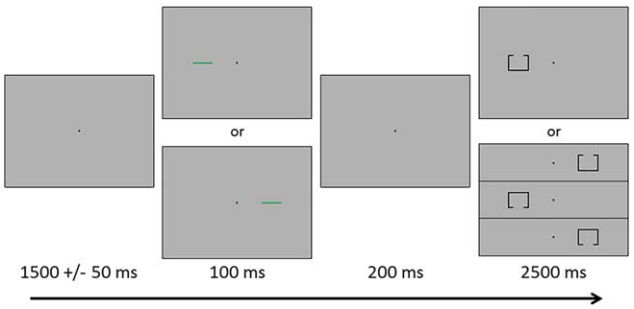


**FIGURE 1** Posner cueing task. A fixation cross was first presented for 1500 ms (±50 ms), and this was followed by a cue (green bar) presented in the left or right visual hemifield for 100 ms. The target stimulus (box with opening) appeared 200 ms after cue offset, in either the left or right visual hemifield, for 2,500 ms. Participants responded as to whether the opening was on the top or bottom of the target. The cue was valid (presented on the same side as the subsequent target) for half of the trials [Color figure can be viewed at wileyonlinelibrary.com]

University of Nebraska Medical Center's Institutional Review Board, which approved the study protocol.

## 2.2 | Experimental paradigm

During MEG recording, participants sat in a nonmagnetic chair within a magnetically shielded room and performed a modified Posner task (Figure 1; Posner, 1980). Participants were instructed to maintain fixation on a centrally presented crosshair throughout the task. Each trial began with the presentation of only the crosshair for 1500 ms (±50 ms). Next, a green bar, serving as the cue, was presented either to the left or right of the crosshair for 100 ms. The cue appeared on a given side 50% of all trials, and could be either valid (i.e., presented on the same side as the subsequent target; 50% of trials) or invalid (i.e., opposite side relative to the target). The target stimulus appeared 200 ms after the cue offset on either the left or right side of the crosshair for 2,500 ms, and consisted of a box with an opening on either the bottom (50% of trials) or top surface. Participants were instructed to respond as to whether the opening was on the bottom (right index finger) or the top (right middle finger) of the box. Each target variant appeared an equal number of times on the left and right sides of the crosshair, and was preceded by an invalid or valid cue an equal number of times. Each trial lasted 4,300 ms (±50 ms) and there were a total of 200 trials (100 valid, 100 invalid), resulting in a total run-time of ~14.5 min.

## 2.3 | MEG data acquisition

Recordings were conducted in a one-layer magnetically-shielded room with active shielding engaged. With an acquisition bandwidth of 0.1–330 Hz, neuromagnetic responses were sampled continuously at 1 kHz using an Elekta MEG system with 306 magnetic sensors (Elekta, Helsinki, Finland). MEG data from each participant were individually corrected for head motion and subjected to noise reduction using the signal space separation method with a temporal extension (Taulu & Simola, 2006; Taulu, Simola, & Kajola, 2005).

## 2.4 | MEG coregistration and structural MRI acquisition and processing

Preceding MEG measurement, four coils were attached to the subject's head and localized, together with the three fiducial points and scalp surface, with a 3-D digitizer (Fastrak 3SF0002, Polhemus Navigator Sciences, Colchester, VT, USA). Once the subject was positioned for MEG recording, an electric current with a unique frequency label (e.g., 322 Hz) was fed to each of the coils. This induced a measurable magnetic field and allowed each coil to be localized in reference to the sensors throughout the recording session. Since coil locations were also known in head coordinates, all MEG measurements could be transformed into a common coordinate system. With this coordinate system, each participant's MEG data were coregistered with their structural T1-weighted neuroanatomical data prior to source space analyses using BESA MRI (Version 2.0; BESA GmbH, Gräfelfing, Germany). These data were acquired with a Philips Achieva 3T X-series scanner using an eight-channel head coil (TR: 8.09 ms; TE: 3.7 ms; field of view: 240 mm; slice thickness: 1 mm; no gap; in-plane resolution: 1.0 × 1.0 mm). All structural MRI data were aligned parallel to the anterior and posterior commissures and transformed into standardized space, along with the functional images, after beamforming (Section 2.6).

## 2.5 | MEG time–frequency transformation and statistics

Cardiac artifacts were removed from the data using signal-space projection (SSP), which was accounted for during source reconstruction (Uusitalo & Ilmoniemi, 1997). The continuous magnetic time series was divided into epochs of 4,000 ms duration, with the onset of the cue being defined as 0 ms and the baseline being defined as the 600 ms preceding cue onset (i.e., −600 to 0 ms). Given our task and epoch design, the target onset occurred at 300 ms. Epochs containing artifacts were rejected based on a fixed threshold method. In brief, for each individual, the distribution of amplitude and gradient values was approximated across all trials, and those trials containing the highest amplitude and/or gradient values relative to the full distribution were rejected by selecting a threshold that excluded extreme values. Importantly, these thresholds were set individually for each participant, as interindividual differences in variables such as head size and proximity to the sensors strongly affects MEG signal amplitude. Additionally, we visually inspected the data to identify trials contaminated with other types of artifacts, such as those produced by muscle tension, and rejected such trials. On average, 84.4 valid and 84.8 invalid trials per participant remained after artifact rejection and were used in subsequent analyses. Artifact-free epochs were transformed into the time–frequency domain using complex demodulation with a resolution of 2 Hz and 25 ms, and the resulting spectral power estimations per sensor were averaged across all trials to generate time–frequency plots of mean spectral density. These sensor-level data were then normalized with respect to baseline power, which was calculated as the mean power during the −600 to 0 ms time period. Of note, this normalization was performed separately for each 2 Hz by 25 ms bin within each spectrogram using the baseline data pertaining to that spectrogram.

The time–frequency windows used for imaging were determined by statistical analysis of the sensor-level spectrograms across all trials (valid + invalid) and gradiometers during the 600 ms time window following target onset. This time window was selected to maximize focus on the attentional reorienting components, while minimizing the impact of other brain responses (e.g., motor) associated with each trial. Each data point (i.e., 2 Hz by 25 ms bin) in the spectrogram was initially evaluated using a mass univariate approach based on the general linear model (GLM). To reduce the risk of false positive results while maintaining reasonable sensitivity, a two stage procedure was followed to control for Type 1 error. In the first stage, one-sample *t*-tests were conducted on each data point and the output spectrogram of *t*-values was thresholded at $p < .05$ to define time–frequency bins containing potentially significant oscillatory deviations across all participants. In stage two, time–frequency bins that survived this threshold were clustered with temporally and/or spectrally neighboring bins that were also significant, and a cluster value was derived by summing all of the *t*-values of all data points in the cluster. Nonparametric permutation testing was then used to derive a distribution of cluster values and the significance level of the observed clusters (from stage one) were tested directly using this distribution (Ernst, 2004; Maris & Oostenveld, 2007). For each comparison, at least 10,000 permutations were computed to build a distribution of cluster values. Based on these analyses, only the time–frequency windows that contained significant oscillatory events across all trials were subjected to the beamforming (i.e., imaging) analysis. Thus, a data-driven approach was utilized for selecting the time–frequency windows to be imaged.

## 2.6 | MEG source imaging and statistics

Cortical networks were imaged through an extension of the linearly constrained minimum variance vector beamformer (Gross et al., 2001; Hillebrand, Singh, Holliday, Furlong, & Barnes, 2005; Van Veen, van Drongelen, Yuchtman, & Suzuki, 1997), which employs spatial filters in the frequency domain to calculate source power for the entire brain volume. The single images were derived from the cross spectral densities of all combinations of MEG gradiometers averaged over the time–frequency range of interest, and the solution of the forward problem for each location on a grid specified by input voxel space. In principle, the beamformer operator generates a spatial filter for each grid point that passes signals without attenuation from the given neural region, while suppressing activity in all other brain areas. The filter properties arise from the forward solution (lead field) for each location on a volumetric grid specified by input voxel space, and from the MEG covariance matrix. Basically, for each voxel, a set of beamformer weights is determined, which amounts to each MEG sensor being allocated a sensitivity weighting for activity in the particular voxel. This set of beamformer weights is the spatial filter unique to the given voxel and this procedure is iterated until such a filter is computed for each voxel in the brain. Activity in each voxel is then determined independently and sequentially to produce a volumetric map of electrical activity with relatively high spatial resolution. In short, this method outputs a power value for each voxel in the brain, determined by a weighted combination of sensor-level time–frequency activity. Following convention, the source power in these images was normalized per participant using a separately averaged prestimulus noise period (i.e., baseline) of equal duration and bandwidth (Hillebrand et al., 2005). MEG preprocessing and imaging used the Brain Electrical Source Analysis (version 6.0) software.

Normalized source power was computed for the selected time-frequency bands over the entire brain volume per participant at 4.0 × 4.0 × 4.0 mm resolution. Each participant's functional images were transformed into standardized space using the transform that was previously applied to the structural images and then spatially resampled. The resulting 3D maps of brain activity reflected activity across both conditions and were averaged across participants to assess the anatomical basis of the significant oscillatory responses identified through the sensor-level analysis. Using these grand-averaged pseudo-*t* maps, we then extracted virtual sensors (i.e., voxel time series) for the peak voxel of each cluster. That is, within each cluster of activity, we identified the voxel displaying the strongest response, and extracted a time series for each condition that corresponded to this voxel. When computing the virtual sensors, we applied the sensor weighting matrix derived from the forward solution to the preprocessed signal vector, which yielded a time series for the specific coordinate. Importantly, we computed virtual sensor time series for each condition (i.e., invalid and valid) separately. Differences in oscillatory activity between conditions were then assessed using timepoint-by-timepoint paired-samples *t*-tests. To control for Type 1 error, the two-stage procedure described above (Section 2.5) was employed, with the criteria of at least 10,000 permutations and a threshold of $p < .05$. Of note, a similar analytical approach has been adopted in previous MEG studies of oscillatory activity (Grent-'t-Jong, Oostenveld, Jensen, Medendorp, & Praamstra, 2013, 2014; Heinrichs-Graham, Hoburg, & Wilson, 2018; Heinrichs-Graham, Kurz, Gehringer, & Wilson, 2017a; Heinrichs-Graham, McDermott, Mills, Coolidge, & Wilson, 2017b; McDermott, Wiesman, Proskovec, Heinrichs-Graham, & Wilson, 2017; Muthukumaraswamy et al., 2013). Additionally, to ensure that transient evoked responses did not contribute to conditional differences, we conducted the same virtual sensor time series analyses while subtracting out evoked activity.

## 2.7 | Functional connectivity analyses

To examine functional connectivity, we computed phase coherence using the voxel time series data and the method described by Lachaux, Rodriguez, Martinerie, and Varela (1999). That is, the same peak voxels utilized in the virtual sensor analyses were used in the connectivity analyses, and for these we used the dominant orientation for each voxel. Specifically, the virtual sensor signals were band-pass filtered at ±1.0 Hz centered on the target frequency, and their convolution was computed using a complex Gabor wavelet. The phase of the convolution was extracted for each time–frequency bin per trial, and the phase relationship between each pair of voxels was evaluated across trials to derive the phase-locking value (PLV). Thus, the PLV reflects the inter-trial variability of the phase relationship between pairs of brain regions as a function of time. Values can range from 0 to 1, with values close to 1 reflecting strong synchronicity (i.e., connectivity) between the two voxel time series, and values close to 0 indicating low connectivity

between the two regions. To examine conditional differences in connectivity, we first baseline-corrected the PLV values for each condition and then conducted paired samples *t*-tests between conditions for each time point. Type 1 error was controlled using the two-stage permutation procedure described above (Section 2.5), with the criteria of at least 10,000 permutations and a threshold of $p < .05$.

## 3 | RESULTS

### 3.1 | Behavioral analysis

Two participants were excluded from all MEG analyses. One was unable to successfully complete the task (i.e., responded at chance levels) and another's MEG data was contaminated with artifacts. The remaining 27 participants performed well on both conditions, accurately responding to 99.11% ($SD = 1.22\%$) of the valid trials and 98.44% ($SD = 1.93\%$) of the invalid trials. This accuracy difference was significant $t(26) = 2.73$, $p = .011$. Additionally, there was a significant difference in reaction time (RT) between conditions $t(26) = -8.77$, $p < .001$, with participants responding more slowly during invalid trials ($M = 1060.73$ ms, $SD = 146.37$ ms) relative to valid trials ($M = 994.36$ ms, $SD = 137.92$ ms). Thus, the validity effect (Vossel et al., 2006) was 66.37 ms on average ($SD = 39.32$).

### 3.2 | Sensor-level analysis

Statistical analysis of the time–frequency spectrograms revealed significant clusters of theta (4–8 Hz), alpha (8–14 Hz), and beta (14–24 Hz) oscillatory activity in gradiometers near the occipital and parietal cortices across all participants and conditions ($p < .001$, corrected; Figure 2). While strong theta and lower alpha visual responses were seen shortly after the onset of the cue, we focused our analyses on oscillatory activity during the target interval, as we were interested in the attentional reorienting processes. During the target interval, significant theta activity began 100 ms after the onset of the target stimulus and tapered off about 250 ms later (i.e., from 400 to 650 ms; $p < .05$, corrected). The time course of alpha and beta activity was much more extended, as significant activity in both bands began at the onset of the target interval and continued for about 600 ms before terminating (i.e., from 300 to 900 ms; $p < .05$, corrected). Thus, three significant time–frequency bins (i.e., theta: 4–8 Hz from 400 to 650 ms; alpha: 8–14 Hz from 300 to 900 ms; and beta: 14–24 Hz from 300 to 900 ms) were identified through these analyses.

### 3.3 | Beamformer analysis

To determine the brain areas generating the significant sensor-level oscillatory responses, each time–frequency bin was imaged using a beamformer. Strong increases in theta activity were observed from 400 to 650 ms in the left prefrontal cortex (PFC), right inferior frontal gyrus (IFG), supplementary motor area (SMA), right frontal eye field (FEF), and bilateral primary visual cortices (Figure 3). In contrast, strong decreases in alpha activity (300–900 ms) were observed in the bilateral superior parietal lobules (SPL), bilateral lateral occipital cortices (LOC), and the left parieto-occipital sulcus (POS; Figure 4). During the same 300–900 ms time period, strong beta decreases were noted in bilateral inferior parietal sulci (IPS), bilateral LOC, and the right supramarginal gyrus (SMG; Figure 5). Finally, decreases in alpha and beta activity were also observed in the left motor hand knob region from 300 to 900 ms. However, these responses were not subjected to the time series analyses, as they were tightly coupled to motor execution processes, and have been extensively detailed elsewhere (Heinrichs-Graham & Wilson, 2015, 2016).

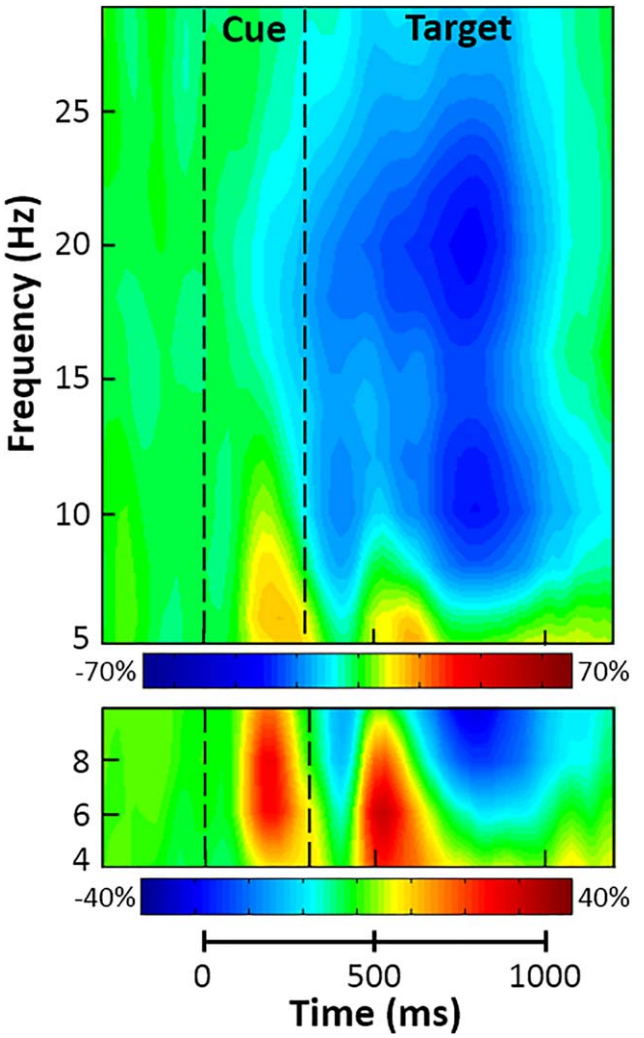


**FIGURE 2** Grand-averaged time–frequency spectrograms for two sensors near the parietal cortices, with time (ms) shown on the *x*-axis and frequency (Hz) denoted on the *y*-axis. Percent power change was computed by dividing the mean power of each time–frequency bin by the respective bin's baseline power (−600 to 0 ms, before cue onset) and multiplying by 100, with the color legends displayed beneath each spectrogram. Data are from two sensors (top: sensor 1832; bottom: sensor 2023), averaged across all trials (i.e., valid and invalid) and participants; the same two sensors were used in each person. Strong decreases in alpha (8–14 Hz) and beta (14–24 Hz) activity were observed at the onset of the target stimulus. Additionally, large increases in theta (4–8 Hz) activity were seen following the cue and later during target processing [Color figure can be viewed at wileyonlinelibrary.com]

In the course of review, one referee inquired about the influence of motor-related responses on our beamformer results, and requested

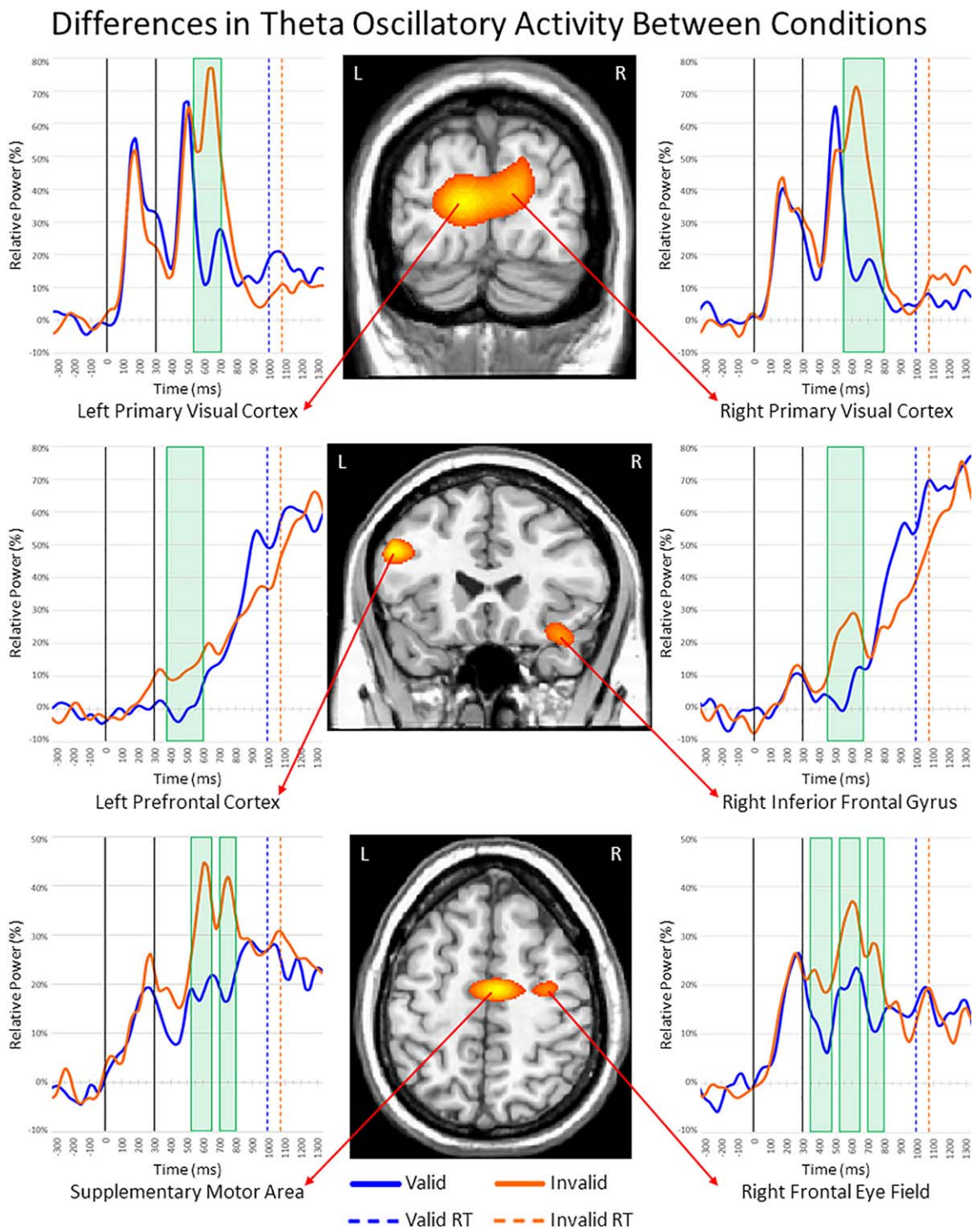


**FIGURE 3** Theta activity during target processing. (Middle) Theta beamformer images were computed across conditions and then averaged across all participants. The output images are shown in pseudo-*t* units following the neurological convention (right hemisphere on right side). Increases in theta activity were observed in the bilateral visual cortices, left prefrontal cortex (PFC), right inferior frontal gyrus (IFG), supplementary motor area (SMA), and right frontal eye fields (FEF). (Left and right) Time courses of theta activity from the peak voxel in each region for valid (blue) and invalid trials (orange). Time periods where significant differences ($p < 0.05$, corrected) were found between conditions are denoted with green boxes. Full legend at the bottom (RT = reaction time) [Color figure can be viewed at wileyonlinelibrary.com]

that a control analysis be performed by shortening the time window which was beamformed (i.e., image from 300 to 700 ms, rather than 300 to 900 ms), thereby reducing possible contamination by motor-related activity. Additionally, the referee questioned whether we observed the well-known visual-hemifield effects on occipital alpha activity (i.e., stronger alpha decreases in the left occipital cortex following target presentation in the right visual hemifield, and vice versa), and requested that we perform an additional control analysis on visual

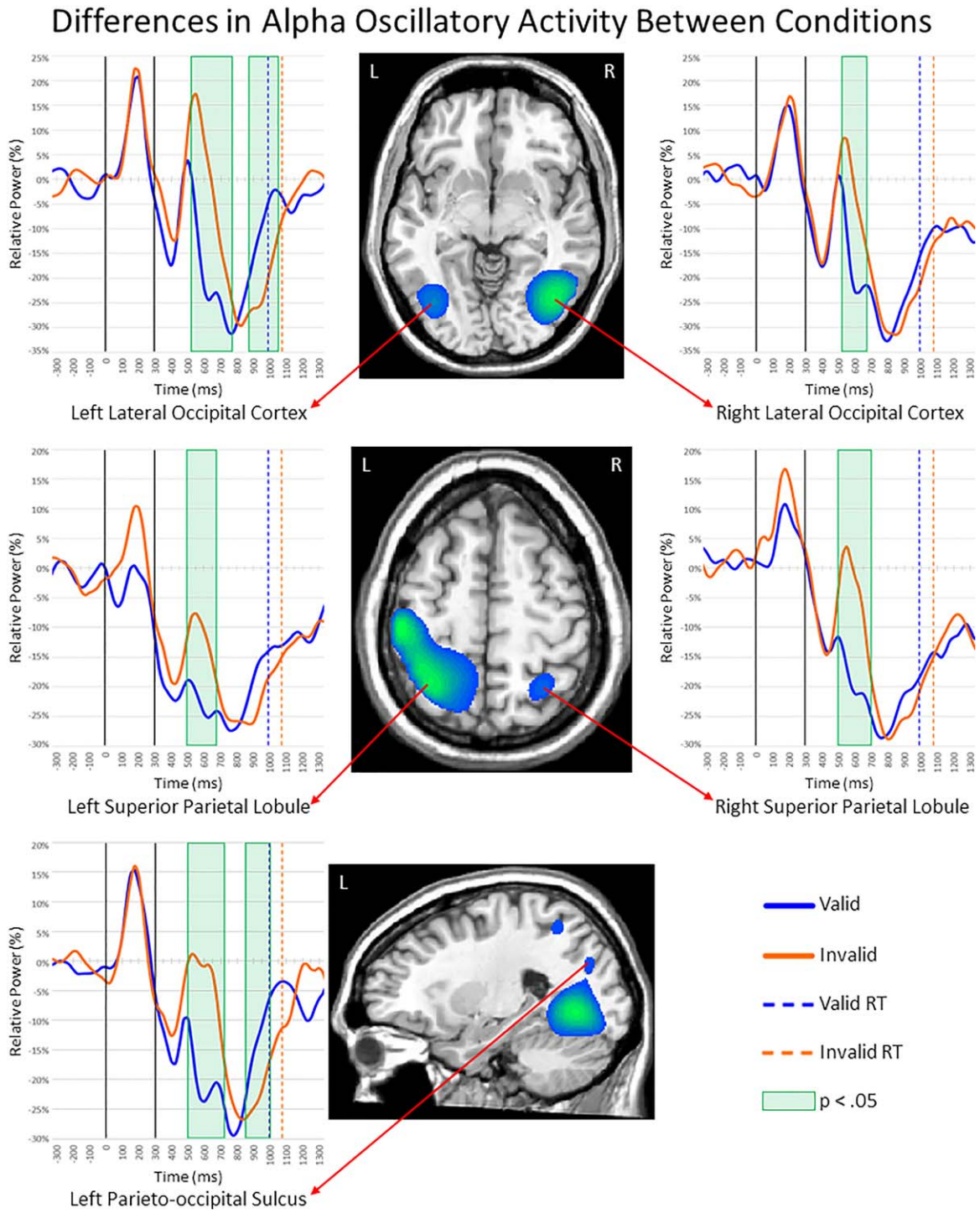


**FIGURE 4** Alpha activity during the first 600 ms of target processing. Layout is similar to Figure 3. (Middle) Alpha beamformer images were computed across conditions and then averaged across all participants. The output images are shown in pseudo-*t* units. As shown, strong decreases in alpha activity were observed in bilateral lateral occipital cortices (LOC), superior parietal lobules (SPL), and the left parieto-occipital sulcus (POS). (Left and Right) Time courses of alpha activity from the peak voxel in each region for valid (blue) and invalid trials (orange). The time periods where significant differences ($p < .05$, corrected) were found between valid and invalid trials are highlighted with green boxes. Note that activity was also detected in left primary motor cortices (middle image) and that the two additional clusters viewable in the bottom image correspond to the left LOC and left SPL. Full legend is shown in the bottom right (RT = reaction time) [Color figure can be viewed at wileyonlinelibrary.com]

laterality. The results of these control analyses are depicted in Supporting Information, Figures S1 and S2. In brief, the motor-response control analysis did not alter our original results, and we replicated the expected visual hemifield-related effects on occipital alpha activity. Additionally, we discuss the contribution of motor-related activity in the Discussion section.

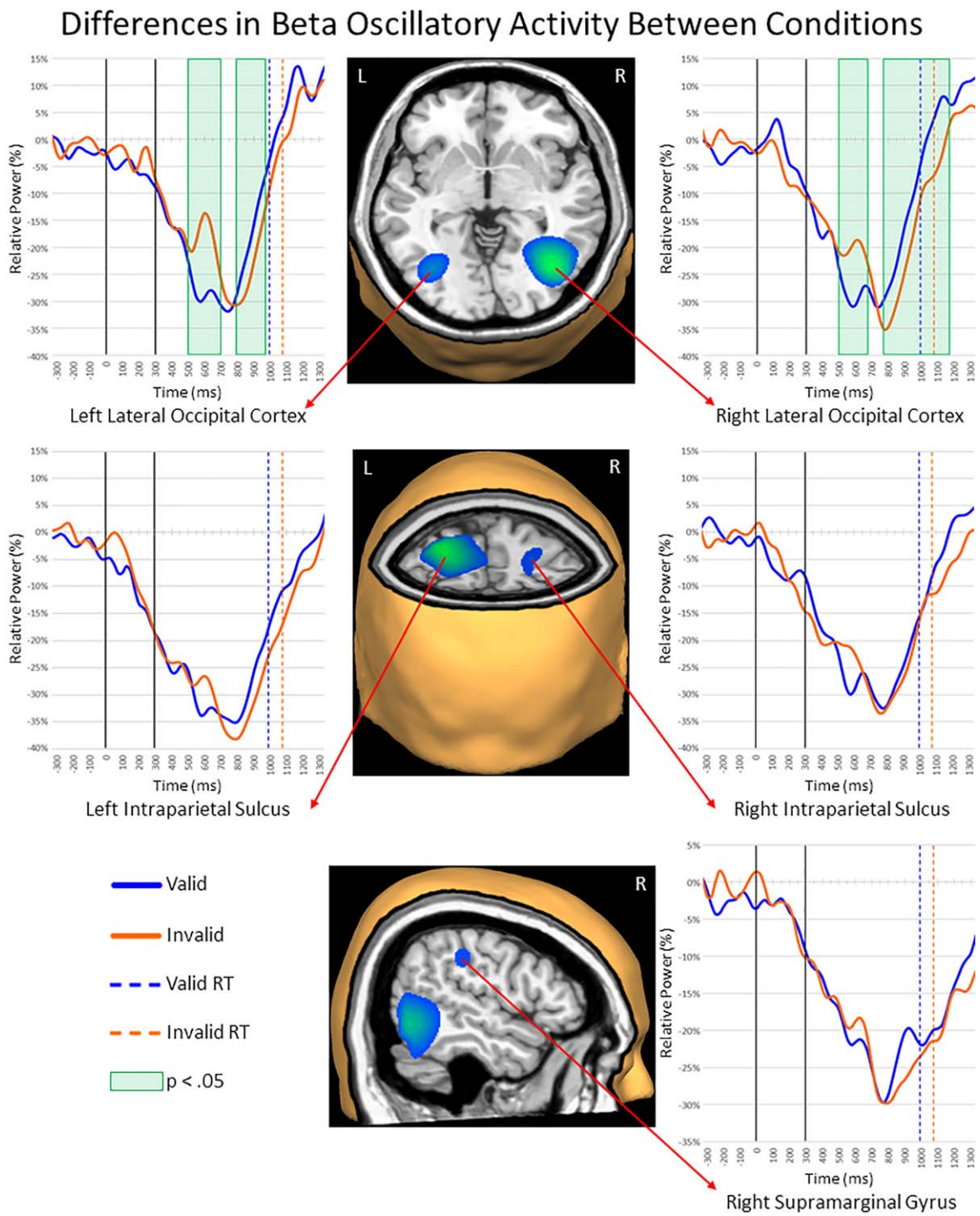


**FIGURE 5** Beta activity during the first 600 ms of target processing. Layout is similar to Figures 3 and 4. (Middle) Beta beamformer images were computed across conditions and then averaged across all participants. The output images are shown in pseudo-t units. Strong decreases in beta activity were observed in bilateral lateral occipital cortices (LOC), intraparietal sulci (IPS), and the right supramarginal gyrus (SMG). (Left and Right) Time courses of beta activity from the peak voxel in each region for valid (blue) and invalid trials (orange). As with Figures 3 and 4, time bins with significant differences ($p < .05$, corrected) between valid and invalid trials are highlighted with green boxes. Legend appears in the bottom left (RT = reaction time) [Color figure can be viewed at wileyonlinelibrary.com]

### 3.4 | Virtual sensor analysis

To quantify the time course of activity in these regions and identify differences in the processing of valid and invalid targets, we extracted virtual sensors for each condition from the peak voxel in the regions described above. Theta activity increased during target processing in bilateral visual cortices across conditions, but was stronger for invalid targets from 525 to 700 ms in left ($p < .05$, corrected) and 550 to 800 ms in right visual cortices ($p < .05$, corrected; Figure 3).

Additionally, the time courses for theta activity in the left PFC and right IFG revealed steady increases throughout target processing in both conditions, with theta activity being significantly stronger during invalid relative to valid targets from 375 to 600 ms in the left PFC ($p < .05$, corrected) and from 450 to 675 ms in the right IFG ($p < .05$, corrected). Similarly, theta activity was stronger in the SMA during invalid compared to valid targets from 525 to 650 ms ($p < .05$, corrected) and from 700 to 800 ms ($p < .05$, corrected), and the same pattern held for the right FEF from 350 to 475 ms ($p < .05$, corrected), 525 to 650 ms ($p < .05$, corrected), and from 700 to 800 ms ($p < .05$, corrected).

In contrast to theta, alpha activity in the bilateral LOC decreased during early target processing across both conditions, briefly rebounded, and then sharply decreased again (Figure 4). This rebound was much stronger for invalid relative to valid targets and this resulted in significantly greater alpha decreases during valid targets in the left LOC from 525 to 775 ms ($p < .05$, corrected) and in the right LOC from 525 to 675 ms ($p < .05$, corrected). Slightly later, the opposite pattern emerged in the left LOC, with significantly greater alpha decreases during invalid relative to valid targets from 875 to 1,050 ms ($p < .05$, corrected). The time series of alpha activity in bilateral SPL showed decreased activity during early target processing across conditions, with significantly stronger decreases during valid relative to invalid targets from 500 to 675 ms in the left SPL ($p < .05$, corrected) and from 500 to 700 ms in the right SPL ($p < .05$, corrected; Figure 4). Finally, alpha activity in the left POS was similar to the LOC, with decreases after target presentation across both conditions, followed by a brief rebound and subsequent decrease. Conditional differences in the left POS started at the peak of the rebound and were observed from 500 to 725 ms ($p < .05$, corrected), reflecting stronger alpha decreases during valid compared to invalid trials, and from 850 to 1,000 ms ($p < .05$, corrected) indicating the opposite pattern of stronger decreases during invalid relative to valid targets.

Large decreases were also observed for beta activity across both conditions in the left and right LOC, with stronger reductions during valid relative to invalid targets from 500 to 700 ms in the left ($p < .05$, corrected; Figure 5) and from 500 to 675 ms in the right LOC ($p < .05$, corrected). In both regions, this effect reversed slightly later in the time course, with beta decreases being stronger during invalid compared to valid trials from 800 to 975 ms in the left LOC ($p < .05$, corrected) and from 775 to 1175 ms in the right homolog ($p < .05$, corrected). In the bilateral IPS (Figure 5), strong decreases in beta activity following target onset were also observed, but there were no differences between valid and invalid trials in either left or right IPS. The same overall pattern was also observed in the right SMG; strong beta decreases following target onset across both conditions, with valid and invalid responses being largely similar. Last, we conducted the same virtual sensor time series analyses with the evoked activity removed, and found strikingly similar results for all aforementioned regions (Supporting Information, Figures S3–S5). Essentially, the direction and nature of significant differences between conditions, and the time-bins in which they occurred were nearly identical across the two approaches. Thus, evoked responses were not a key contributor to our main findings.

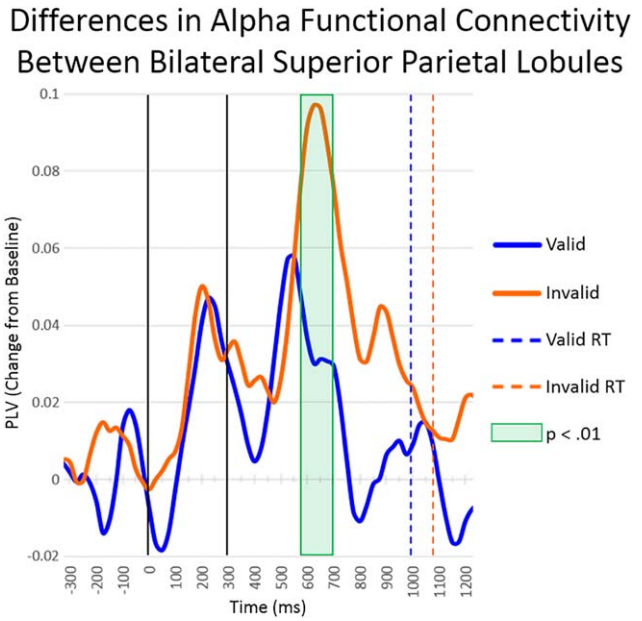


**FIGURE 6** Dynamic functional connectivity between left and right superior parietal lobules (SPL). Time series of alpha-frequency phase-locking between left and right SPL for the valid condition and invalid condition are shown, with the baseline-corrected phase-locking value (PLV) on the *y*-axis and time on the *x*-axis. Significant differences ($p < .05$, corrected) in functional connectivity between conditions are highlighted with a green box. Basically, connectivity was stronger between right and left SPL's during invalid relative to valid trials from 575 to 700 ms. Legend appears on the right (RT = reaction time) [Color figure can be viewed at wileyonlinelibrary.com]

### 3.5 | Functional connectivity analysis

To investigate whether functional connectivity between the previously identified regions changed during target processing, we calculated the PLV for each condition separately and baseline corrected the resulting data. After controlling for relative power at both sources (Brookes et al., 2011), our analyses revealed significantly stronger connectivity in the alpha band between the left and right SPL from 575 to 700 ms during the processing of invalid relative to valid targets ($p < .05$, corrected; Figure 6). Connectivity between other pairs of brain regions did not statistically differ between valid and invalid target processing.

## 4 | DISCUSSION

In this study, we employed high-density MEG and the Posner task (Posner, 1980) to characterize the dynamics of oscillatory activity and functional connectivity serving the reorienting of attention. Our analyses revealed a complex pattern of frequency-specific responses within, and dynamic functional connectivity between, regions of the DAN and VAN. As hypothesized, across conditions the time series revealed substantial increases in theta activity (4–8 Hz) and decreases in alpha (8–14 Hz) and beta (14–24 Hz) activity within attention networks. The increases in theta were typically stronger during the processing of invalid targets in both attention networks, while the decreases in alpha

and beta were generally stronger during the early processing of valid relative to invalid targets, with the opposite pattern emerging during later processing for some regions. Finally, functional connectivity in the alpha band between nodes of the DAN was greater during invalid target processing. The implications of these results are discussed below.

While the Posner paradigm is a classic task utilized for assessing the reorienting of attention, it is important to recognize the numerous sub-processes that occur during performance of the task. One such sub-process would be the initial encoding of the target stimulus, which would require the swift recruitment of the visual cortices after target presentation. As such, the strong increases in theta activity we observed in bilateral visual cortices quickly after target presentation may reflect such an encoding mechanism. This interpretation is further bolstered by previous work which suggests that theta activity within striate regions reflects the early sensory encoding of target stimuli during visual attention (Fries, 2015; Landau & Fries, 2012). Following the encoding of the visual stimulus, higher level visual processing of the target would be expected in downstream lateral extrastriate regions, known to contain receptive fields for specific stimulus properties (e.g., shape, color, and location). The strong decreases in alpha and beta activity observed in bilateral LOC are likely neural candidates in this regard. The engagement of these regions during visual attention tasks has been widely reported (Corbetta & Shulman, 2002; Giesbrecht, Weissman, Woldorff, & Mangun, 2006; Hopfinger, Buonocore, & Mangun, 2000; Kastner & Ungerleider, 2000). Furthermore, neurophysiological studies have demonstrated similar reductions in occipital alpha activity during the covert orienting of visuospatial attention (Deiber et al., 2013; Frey, Ruhnau, & Weisz, 2015), and the functional significance of alpha activity accords well with an active orienting mechanism. That is, decreased alpha activity within a region is thought to signify the active engagement of that region during cognitive processes (Klimesch, 2012; Klimesch et al., 2007), and similar proposals have been made regarding beta band modulations (Neuper & Pfurtscheller, 2001). In congruence with this interpretation, simultaneous EEG-fMRI research has demonstrated negative associations between alpha/beta activity and fMRI activation during cognitive tasks (Michels et al., 2010; Murta, Leite, Carmichael, Figueiredo, & Lemieux, 2015; Scheeringa et al., 2011). Taken together, the theta activity seen in bilateral visual cortices likely reflects early coding mechanisms, while alpha activity observed in bilateral LOC likely indicate processing of specific features inherent to the target stimuli. The dynamic differences between valid and invalid targets within these striate and extrastriate regions may indicate more effortful processing during invalid trials, and/or a temporal shift in processing within this area due to the additional time cost of reorienting attention to the visual stimulus.

Beyond bottom–up visual subprocesses, performance of the Posner task also requires top–down control processes, enacted by the DAN, to select goal-relevant information (Corbetta et al., 2008; Corbetta & Shulman, 2002; Hopfinger et al., 2000; Kastner & Ungerleider, 2000). The decreased alpha activity we observed in bilateral SPL may reflect these top–down attentional control mechanisms, and our findings accord well with previous research that also implicates bilateral SPL in such processes (Corbetta, Kincade, Ollinger, McAvoy, & Shulman, 2000; Corbetta, Kincade, & Shulman, 2002; Corbetta et al., 2008; Corbetta & Shulman, 2002; Petersen & Posner, 2012; Shulman & Corbetta, 2012; Vossel et al., 2014). In essence, these data support the well-known (Bressler, Tang, Sylvester, Shulman, & Corbetta, 2008; Capotosto, Babiloni, Romani, & Corbetta, 2009; Hopfinger et al., 2000; Ruff et al., 2008; Saalmann, Pigarev, & Vidyasagar, 2007; Sylvester, Shulman, Jack, & Corbetta, 2007; Vossel, Weidner, Driver, Friston, & Fink, 2012) biased competition model of attention (Desimone & Duncan, 1995). As for differences between conditions, the aforementioned alpha and beta activity displayed a similar pattern, such that stronger decreases were observed for valid relative to invalid targets during early target processing. Slightly later, the reverse pattern was observed for alpha, beta, and theta occipital responses, which bolsters the argument that the SPL dynamics serve top–down attentional processes. While one would expect these selection mechanisms to be engaged during the processing of all target stimuli, the disengagement of attention from the location of an invalid cue would be necessary before attention could be reoriented toward the alternate location, and this would plausibly cause a delay in the engagement of top–down mechanisms for invalid targets. Indeed, this pattern was demonstrated in the aforementioned regions. The delayed reaction times seen for invalid targets further supports this conclusion, as does our data's alignment with previous work (Chica, Bartolomeo, & Lupianez, 2013; Corbetta et al., 2000, 2002, 2008; Corbetta & Shulman, 2002; Deiber et al., 2013; Frey et al., 2015; Hopfinger et al., 2000).

Interestingly, we also observed stronger functional connectivity in the alpha band between bilateral SPL during invalid relative to valid targets. Complementary to these results, fMRI studies have demonstrated functional connectivity between bilateral parietal regions during attentional orienting (He et al., 2007), and both left and right parietal regions have been implicated in top–down control of covert spatial attention (Capotosto, Babiloni, Romani, & Corbetta, 2012; Vossel et al., 2012). As such, the increased functional connectivity observed in the current study may represent interareal communication serving attentional control processes. The idea of interareal communication via coupled oscillations has been supported by previous studies in other domains (Engel, Fries, & Singer, 2001; Fries, 2005, 2015; Keil, Pomper, & Senkowski, 2016; von Stein & Sarnthein, 2000; Womelsdorf & Fries, 2007).

Further recruitment of the DAN was evidenced in our data as increased theta activity in the FEF. This was not surprising given that multiple studies have demonstrated this region's involvement in top–down control of sensory regions and its coupling with IPS regions during visuospatial attention (Armstrong, Chang, & Moore, 2009; Bressler et al., 2008; Capotosto et al., 2009; Corbetta & Shulman, 2002; Petersen & Posner, 2012; Vossel et al., 2012). Additionally, in congruence with our results, previous work has reported enhanced FEF responses during the reorienting of attention to visual stimuli (Corbetta et al., 2008; Vossel et al., 2006).

In addition to bottom–up and top–down subprocesses, there remains the subprocesses underlying reorienting attention itself. One necessary component in this regard is the disengagement of attention from invalidly cued locations, accomplished via the VAN, so that it may

be redirected to the new target location (Corbetta et al., 2008; Corbetta & Shulman, 2002; Petersen & Posner, 2012). Our observation of increased theta activity in the right IFG during early processing of invalid targets may reflect this mechanism. This interpretation aligns with previous research that demonstrated strong activation of the VAN during attentional reorienting, which was proposed to act as a "circuit-breaker" for the DAN when attention needed to be reallocated to a new spatial location (Corbetta et al., 2008; Corbetta & Shulman, 2002; Petersen & Posner, 2012). A complementary subprocess in this regard would be the rapid adjustment of the neural resources underlying visuospatial attention during the early processing of invalid targets via executive control regions. The increased theta activity found in the PFC may constitute such a mechanism, as the PFC is thought to belong to a network of regions involved in rapid and adaptive executive control (Dosenbach, Fair, Cohen, Schlaggar, & Petersen, 2008). In sum, we propose that the oscillatory theta responses observed in frontal regions may be critical to the processing of invalid targets, and potentially serve active reorienting mechanisms.

Last, as the Posner task incorporates a behavioral response, subprocesses serving response selection would be expected in motor-related regions. The theta responses in the SMA may constitute this process, as the SMA is thought to be critical to response selection and preparation during cued attention tasks (Chica et al., 2013; Corbetta et al., 2002; Hopfinger et al., 2000). Furthermore, our data are consistent with previous research demonstrating this region's involvement in visuospatial attention (Chica et al., 2013; Corbetta et al., 2002; Hopfinger et al., 2000; Kincade, Abrams, Astafiev, Shulman, & Corbetta, 2005; Levy & Wagner, 2011; Mayer, Seidenberg, Dorflinger, & Rao, 2004; Mayer, Harrington, Adair, & Lee, 2006; Vossel et al., 2012), and complementary to our results, stronger activation of the SMA following invalid target presentation has been reported in fMRI studies (Levy & Wagner, 2011; Mayer et al., 2006). Essentially, a valid cue may facilitate response preparedness to a subsequent target, while an invalid cue may require greater motor preparation to reorient toward the target.

To our surprise, the strong decreases in beta activity that we observed in the right SMG and bilateral IPS did not differ between conditions, suggesting that these brain regions serve a more general attention mechanism that is less affected by reorienting. One such mechanism could be attentional alerting, and this interpretation aligns with previous studies that have demonstrated the inclusion of bilateral inferior parietal areas in an alerting network (Fan et al., 2005, 2007; Perin, Godefroy, Fall, & de Marco, 2010; Xuan et al., 2016).

Finally, with regards to the impact of motor-related responses on our results, at a reviewer's request we imaged the beta response using a shorter time window (i.e., from 300 to 700 ms) than that utilized in our original analysis (i.e., from 300 to 900 ms) to reduce possible contamination by motor-related activity. While assessing the contribution of motor-related activity was not a goal of the present study, our laboratory has a history of investigating the oscillatory signature of motor control (Arpin et al., 2017; Heinrichs-Graham, Arpin, & Wilson, 2016; Heinrichs-Graham et al., 2014, 2018, 2017a; Heinrichs-Graham, Santamaria, Gendelman, & Wilson, 2017c; Heinrichs-Graham & Wilson, 2015, 2016; Kurz, Becker, Heinrichs-Graham, & Wilson, 2014; Kurz et al., 2016; Kurz, Proskovec, Gehringer, Heinrichs-Graham, & Wilson, 2017; Wilson et al., 2013; Wilson, Heinrichs-Graham, & Becker, 2014), and we are acquainted with the impact that motor-related responses can have on cognitive paradigms. As such, we anticipated that beamforming a shorter time window would result in a global reduction in beta power throughout the cortex. Essentially, reducing the window width would result in only a portion of the beta response depicted in Figure 2 being imaged, rather than the full response. As the power in our beamformer images is collapsed across the time window, shortening the time window in this way would effectively exclude time periods containing strong oscillatory activity (i.e., that observed within the 700–900 ms range), which would likely attenuate not only any motor-related beta responses in left M1, but also those beta responses identified in other brain regions. As the results in Supporting Information, Figure S1 demonstrate, this was indeed the outcome. We observed a global reduction in beta power across the cortex when employing the shorter time window. Importantly, after adjusting the pseudo-*t* threshold to account for the overall lower beta power across the whole-brain map, nearly identical beta responses were found using the shorter time window. These results provide convincing evidence that the motor-related oscillatory responses did not significantly impact our original results.

Despite the breadth of information provided by our study, it was not without limitations. For example, our study focused on younger adults and healthy aging has been associated with declines in some cognitive functions (Park et al., 2002), including deficits in the disengagement of attention from spatial cues (Erel & Levy, 2016; Langley, Friesen, Saville, & Ciernia, 2011). Additionally, previous studies have demonstrated age-related differences in the neural activity underlying attention-demanding cognitive operations (Grady, 2012; Proskovec, Heinrichs-Graham, & Wilson, 2016; Wilson, Heinrichs-Graham, Proskovec, & McDermott, 2016). As such, future studies should investigate the effects of aging on the dynamics of oscillatory activity serving attentional reorienting. It is also important to note that our strongest conclusions pertain to those drawn from the conditional differences that we observed, as cue validity was the variable that was manipulated in our experimental design. Of course, conclusions regarding the functional significance of the oscillatory responses that we observed within specific regions relied heavily on previous research, and thus should be considered in this context. While it is arguably impossible to directly manipulate all of the subprocesses contributing to the task within one experiment, future studies should independently examine these cognitive subprocesses to more conclusively identify which brain regions are responsible for each aspect of attentional reorientation. Finally, the analysis pipeline that we adopted was specific in that we determined our regions of interest by imaging the significant time–frequency bins identified through the sensor-level analysis, and then extracted the virtual sensor time series for the whole epoch from each region. This approach was preferred, as it enabled the dynamics within each region to be identified and tested for conditional differences. However, of note, a small number of the observed conditional differences in alpha and beta occipital activity extended beyond the time window

which was originally imaged, and these should be interpreted with caution.

## 5 | CONCLUSIONS

To close, our results provide critical new insight into the spectrally specific dynamics of oscillatory activity and functional connectivity underlying the reorienting of attention. Specifically, the current data indicate that dynamics in the alpha rhythm across nodes of the DAN may serve top–down attentional processes, while theta activity within the frontal cortices appears to be more connected to the active reorienting of attention. In contrast, beta activity within dorsal and ventral parietal regions may underlie attentional alerting mechanisms.

### ACKNOWLEDGMENTS

This work was supported by NIH grant R01 MH103220 (TWW) and NSF grant #1539067 (TWW). This work was also supported by a Research Support Fund grant from the Nebraska Health System and the University of Nebraska Medical Center (TWW).

### FINANCIAL DISCLOSURE

No conflicts of interest, financial or otherwise, are declared by the authors.

### ORCID

*Amy L. Proskovec* http://orcid.org/0000-0001-7660-0318
*Elizabeth Heinrichs-Graham* http://orcid.org/0000-0002-7914-5258
*Alex I. Wiesman* http://orcid.org/0000-0003-0917-1570
*Timothy J. McDermott* http://orcid.org/0000-0002-8860-0646
*Tony W. Wilson* http://orcid.org/0000-0002-5053-8306

### REFERENCES

Armstrong, K. M., Chang, M. H., & Moore, T. (2009). Selection and maintenance of spatial information by frontal eye field neurons. *J Neurosci*, *29*, 15621–15629.

Arpin, D. J., Heinrichs-Graham, E., Gehringer, J. E., Zabad, R., Wilson, T. W., & Kurz, M. J. (2017). Altered sensorimotor cortical oscillations in individuals with multiple sclerosis suggests a faulty internal model. *Hum Brain Mapp*, *38*, 4009–4018.

Bressler, S. L., Tang, W., Sylvester, C. M., Shulman, G. L., & Corbetta, M. (2008). Top-down control of human visual cortex by frontal and parietal cortex in anticipatory visual spatial attention. *The Journal of Neuroscience : The Official Journal of the Society for Neuroscience*, *28*, 10056–10061.

Brookes, M. J., Hale, J. R., Zumer, J. M., Stevenson, C. M., Francis, S. T., … Nagarajan, S. S. (2011). Measuring functional connectivity using MEG: methodology and comparison with fcMRI. *Neuroimage*, *56*, 1082–1104.

Busch, N. A., & VanRullen, R. (2010). Spontaneous EEG oscillations reveal periodic sampling of visual attention. *Proceedings of the National Academy of Sciences of the United States of America U S A*, *107*, 16048–16053.

Capotosto, P., Babiloni, C., Romani, G. L., & Corbetta, M. (2009). Frontoparietal cortex controls spatial attention through modulation of anticipatory alpha rhythms. *The Journal of Neuroscience : The Official Journal of the Society for Neuroscience*, *29*, 5863–5872.

Capotosto, P., Babiloni, C., Romani, G. L., & Corbetta, M. (2012). Differential contribution of right and left parietal cortex to the control of spatial attention: a simultaneous EEG-rTMS study. *Cerebral Cortex (New York, N. Y. : 1991)*, *22*, 446–454.

Chica, A. B., Bartolomeo, P., & Lupianez, J. (2013). Two cognitive and neural systems for endogenous and exogenous spatial attention. *Behav Brain Res*, *237*, 107–123.

Corbetta, M., Kincade, J. M., Ollinger, J. M., McAvoy, M. P., & Shulman, G. L. (2000). Voluntary orienting is dissociated from target detection in human posterior parietal cortex. *Nature Neuroscience*, *3*, 292–297.

Corbetta, M., Kincade, J. M., & Shulman, G. L. (2002). Neural systems for visual orienting and their relationships to spatial working memory. *Journal of Cognitive Neuroscience*, *14*, 508–523.

Corbetta, M., Patel, G., & Shulman, G. L. (2008). The reorienting system of the human brain: from environment to theory of mind. *Neuron*, *58*, 306–324.

Corbetta, M., & Shulman, G. L. (2002). Control of goal-directed and stimulus-driven attention in the brain. *Nature Reviews. Neuroscience*, *3*, 201–215.

Cosmelli, D., Lopez, V., Lachaux, J. P., Lopez-Calderon, J., Renault, B., … Aboitis, F. (2011). Shifting visual attention away from fixation is specifically associated with alpha band activity over ipsilateral parietal regions. *Psychophysiology*, *48*, 312–322.

Daitch, A. L., Sharma, M., Roland, J. L., Astafiev, S. V., Bundy, D. T., … Corbetta, M. (2013). Frequency-specific mechanism links human brain networks for spatial attention. *Proceedings of the National Academy of Sciences of the United States of America U S A*, *110*, 19585–19590.

Deiber, M. P., Ibanez, V., Missonnier, P., Rodriguez, C., & Giannakopoulos, P. (2013). Age-associated modulations of cerebral oscillatory patterns related to attention control. *Neuroimage*, *82*, 531–546.

Desimone, R., & Duncan, J. (1995). Neural mechanisms of selective visual attention. *Annual Review of Neuroscience*, *18*, 193–222.

Doricchi, F., Macci, E., Silvetti, M., & Macaluso, E. (2010). Neural correlates of the spatial and expectancy components of endogenous and stimulus-driven orienting of attention in the Posner task. *Cerebral Cortex (New York, N.Y. : 1991)*, *20*, 1574–1585.

Dosenbach, N. U., Fair, D. A., Cohen, A. L., Schlaggar, B. L., & Petersen, S. E. (2008). A dual-networks architecture of top-down control. *Trends in Cognitive Sciences*, *12*, 99–105.

Dugue, L., Roberts, M., & Carrasco, M. (2016). Attention Reorients Periodically. *Curr Biol*, *26*, 1595–1601.

Engel, A. K., Fries, P., & Singer, W. (2001). Dynamic predictions: oscillations and synchrony in top-down processing. *Nature Reviews. Neuroscience*, *2*, 704–716.

Erel, H., & Levy, D. A. (2016). Orienting of visual attention in aging. *Neuroscience and Biobehavioral Reviews*, *69*, 357–380.

Ernst, M. D. (2004). Permutation methods: A basis for exact inference. *Stat Sci*, *19*, 676–685.

Fan, J., Byrne, J., Worden, M. S., Guise, K. G., McCandliss, B. D., Fossella, J., & Posner, M. I. (2007). The relation of brain oscillations to attentional networks. *The Journal of Neuroscience : The Official Journal of the Society for Neuroscience*, *27*, 6197–6206.

Fan, J., McCandliss, B. D., Fossella, J., Flombaum, J. I., & Posner, M. I. (2005). The activation of attentional networks. *Neuroimage*, *26*, 471–479.

Frey, J. N., Ruhnau, P., & Weisz, N. (2015). Not so different after all: The same oscillatory processes support different types of attention. *Brain Research*, *1626*, 183–197.

Fries, P. (2005). A mechanism for cognitive dynamics: neuronal communication through neuronal coherence. *Trends in Cognitive Sciences*, *9*, 474–480.

Fries, P. (2015). Rhythms for Cognition: Communication through Coherence. *Neuron*, *88*, 220–235.

Giesbrecht, B., Weissman, D. H., Woldorff, M. G., & Mangun, G. R. (2006). Pre-target activity in visual cortex predicts behavioral performance on spatial and feature attention tasks. *Brain Research*, *1080*, 63–72.

Grady, C. (2012). The cognitive neuroscience of ageing. *Nature Reviews. Neuroscience*, *13*, 491–505.

Grent-'t-Jong, T., Oostenveld, R., Jensen, O., Medendorp, W. P., & Praamstra, P. (2013). Oscillatory dynamics of response competition in human sensorimotor cortex. *Neuroimage*, *83*, 27–34.

Grent-'t-Jong, T., Oostenveld, R., Jensen, O., Medendorp, W. P., & Praamstra, P. (2014). Competitive interactions in sensorimotor cortex: Oscillations express separation between alternative movement targets. *Journal of Neurophysiology*, *112*, 224–232.

Gross, J., Kujala, J., Hamalainen, M., Timmermann, L., Schnitzler, A., & Salmelin, R. (2001). Dynamic imaging of coherent sources: Studying neural interactions in the human brain. *Proc Natl Acad Sci U S A*, *98*, 694–699.

He, B. J., Snyder, A. Z., Vincent, J. L., Epstein, A., Shulman, G. L., & Corbetta, M. (2007). Breakdown of functional connectivity in frontoparietal networks underlies behavioral deficits in spatial neglect. *Neuron*, *53*, 905–918.

Heinrichs-Graham, E., Arpin, D. J., & Wilson, T. W. (2016). Cue-related temporal factors modulate movement-related beta oscillatory activity in the human motor circuit. *Journal of Cognitive Neuroscience*, *28*, 1039–1051.

Heinrichs-Graham, E., Hoburg, J. M., & Wilson, T. W. (2018). The peak frequency of motor-related gamma oscillations is modulated by response competition. *Neuroimage*, *165*, 27–34.

Heinrichs-Graham, E., Kurz, M. J., Gehringer, J. E., & Wilson, T. W. (2017a). The functional role of post-movement beta oscillations in motor termination. *Brain Struct Funct*, *222*, 3075–3086.

Heinrichs-Graham, E., McDermott, T. J., Mills, M. S., Coolidge, N. M., & Wilson, T. W. (2017b). Transcranial direct-current stimulation modulates offline visual oscillatory activity: A magnetoencephalography study. *Cortex*, *88*, 19–31.

Heinrichs-Graham, E., Santamaria, P. M., Gendelman, H. E., & Wilson, T. W. (2017c). The cortical signature of symptom laterality in Parkinson's disease. *Neuroimage Clin*, *14*, 433–440.

Heinrichs-Graham, E., & Wilson, T. W. (2015). Coding complexity in the human motor circuit. *Human Brain Mapping*, *36*, 5155–5167.

Heinrichs-Graham, E., & Wilson, T. W. (2016). Is an absolute level of cortical beta suppression required for proper movement? Magnetoencephalographic evidence from healthy aging. *Neuroimage*, *134*, 514–521.

Heinrichs-Graham, E., Wilson, T. W., Santamaria, P. M., Heithoff, S. K., Torres-Russotto, D., … Gendelman, H. E. (2014). Neuromagnetic evidence of abnormal movement-related beta desynchronization in Parkinson's disease. *Cerebral Cortex (New York, N.Y. : 1991)*, *24*, 2669–2678.

Hillebrand, A., Singh, K. D., Holliday, I. E., Furlong, P. L., & Barnes, G. R. (2005). A new approach to neuroimaging with magnetoencephalography. *Human Brain Mapping*, *25*, 199–211.

Hopfinger, J. B., Buonocore, M. H., & Mangun, G. R. (2000). The neural mechanisms of top-down attentional control. *Nature Neuroscience*, *3*, 284–291.

Indovina, I., & Macaluso, E. (2007). Dissociation of stimulus relevance and saliency factors during shifts of visuospatial attention. *Cerebral Cortex (New York, N.Y. : 1991)*, *17*, 1701–1711.

Kastner, S., & Ungerleider, L. G. (2000). Mechanisms of visual attention in the human cortex. *Annual Review of Neuroscience*, *23*, 315–341.

Keil, J., Pomper, U., & Senkowski, D. (2016). Distinct patterns of local oscillatory activity and functional connectivity underlie intersensory attention and temporal prediction. *Cortex; a Journal Devoted to the Study of the Nervous System and Behavior*, *74*, 277–288.

Kincade, J. M., Abrams, R. A., Astafiev, S. V., Shulman, G. L., & Corbetta, M. (2005). An event-related functional magnetic resonance imaging study of voluntary and stimulus-driven orienting of attention. *The Journal of Neuroscience: The Official Journal of the Society for Neuroscience*, *25*, 4593–4604.

Klimesch, W. (2012). alpha-band oscillations, attention, and controlled access to stored information. *Trends in Cognitive Sciences*, *16*, 606–617.

Klimesch, W., Sauseng, P., & Hanslmayr, S. (2007). EEG alpha oscillations: the inhibition-timing hypothesis. *Brain Research Reviews*, *53*, 63–88.

Kurz, M. J., Becker, K. M., Heinrichs-Graham, E., & Wilson, T. W. (2014). Neurophysiological abnormalities in the sensorimotor cortices during the motor planning and movement execution stages of children with cerebral palsy. *Develop Med Child Neurol*, *56*, 1072–1077.

Kurz, M. J., Proskovec, A. L., Gehringer, J. E., Becker, K. M., Arpin, D. J., Heinrichs-Graham, E., & Wilson, T. W. (2016). Developmental trajectory of beta cortical oscillatory activity during a knee motor task. *Brain Top*, *29*, 824–833.

Kurz, M. J., Proskovec, A. L., Gehringer, J. E., Heinrichs-Graham, E., & Wilson, T. W. (2017). Children with cerebral palsy have altered oscillatory activity in the motor and visual cortices during a knee motor task. *Neuroimage. Clinical*, *15*, 298–305.

Lachaux, J. P., Rodriguez, E., Martinerie, J., & Varela, F. J. (1999). Measuring phase synchrony in brain signals. *Human Brain Mapping*, *8*, 194–208.

Landau, A. N., & Fries, P. (2012). Attention samples stimuli rhythmically. *Current Biology : Cb*, *22*, 1000–1004.

Langley, L. K., Friesen, C. K., Saville, A. L., & Ciernia, A. T. (2011). Timing of reflexive visuospatial orienting in young, young-old, and old-old adults. *Attention, Perception &Amp; Psychophysics*, *73*, 1546–1561.

Leitao, J., Thielscher, A., Tunnerhoff, J., & Noppeney, U. (2015). Concurrent TMS-fMRI Reveals Interactions between Dorsal and Ventral Attentional Systems. *The Journal of Neuroscience : The Official Journal of the Society for Neuroscience*, *35*, 11445–11457.

Levy, B. J., & Wagner, A. D. (2011). Cognitive control and right ventrolateral prefrontal cortex: reflexive reorienting, motor inhibition, and action updating. *Annals of the New York Academy of Sciences*, *1224*, 40–62.

Macaluso, E., & Patria, F. (2007). Spatial re-orienting of visual attention along the horizontal or the vertical axis. *Experimental Brain Research*, *180*, 23–34.

Maris, E., & Oostenveld, R. (2007). Nonparametric statistical testing of EEG- and MEG-data. *Journal of Neuroscience Methods*, *164*, 177–190.

Mayer, A. R., Harrington, D., Adair, J. C., & Lee, R. (2006). The neural networks underlying endogenous auditory covert orienting and reorienting. *Neuroimage*, *30*, 938–949.

Mayer, A. R., Seidenberg, M., Dorflinger, J. M., & Rao, S. M. (2004). An event-related fMRI study of exogenous orienting: supporting evidence for the cortical basis of inhibition of return?. *Journal of Cognitive Neuroscience*, *16*, 1262–1271.

McDermott, T. J., Wiesman, A. I., Proskovec, A. L., Heinrichs-Graham, E., & Wilson, T. W. (2017). Spatiotemporal oscillatory dynamics of visual selective attention during a flanker task. *Neuroimage*, *156*, 277–285.

Michels, L., Bucher, K., Luchinger, R., Klaver, P., Martin, E., Jeanmonod, D., & Brandeis, D. (2010). Simultaneous EEG-fMRI during a working memory task: modulations in low and high frequency bands. *PLoS One*, *5*, e10298.

Murta, T., Leite, M., Carmichael, D. W., Figueiredo, P., & Lemieux, L. (2015). Electrophysiological correlates of the BOLD signal for EEG-informed fMRI. *Human Brain Mapping*, *36*, 391–414.

Muthukumaraswamy, S. D., Myers, J. F., Wilson, S. J., Nutt, D. J., Lingford-Hughes, A., Singh, K. D., & Hamandi, K. (2013). The effects of elevated endogenous GABA levels on movement-related network oscillations. *Neuroimage*, *66*, 36–41.

Nagata, Y., Bayless, S. J., Mills, T., & Taylor, M. J. (2012). Spatio-temporal localisation of attentional orienting to gaze and peripheral cues. *Brain Research*, *1439*, 44–53.

Neuper, C., & Pfurtscheller, G. (2001). Event-related dynamics of cortical rhythms: frequency-specific features and functional correlates. *International Journal of Psychophysiology : Official Journal of the International Organization of Psychophysiology*, *43*, 41–58.

Park, D. C., Lautenschlager, G., Hedden, T., Davidson, N. S., Smith, A. D., & Smith, P. K. (2002). Models of visuospatial and verbal memory across the adult life span. *Psychology and Aging*, *17*, 299–320.

Perin, B., Godefroy, O., Fall, S., & de Marco, G. (2010). Alertness in young healthy subjects: an fMRI study of brain region interactivity enhanced by a warning signal. *Brain and Cognition*, *72*, 271–281.

Petersen, S. E., & Posner, M. I. (2012). The attention system of the human brain: 20 years after. *Annual Review of Neuroscience*, *35*, 73–89.

Posner, M. I. (1980). Orienting of attention. *The Quarterly Journal of Experimental Psychology*, *32*, 3–25.

Proskovec, A. L., Heinrichs-Graham, E., & Wilson, T. W. (2016). Aging modulates the oscillatory dynamics underlying successful working memory encoding and maintenance. *Human Brain Mapping*, *37*, 2348–2361.

Rihs, T. A., Michel, C. M., & Thut, G. (2009). A bias for posterior alpha-band power suppression versus enhancement during shifting versus maintenance of spatial attention. *Neuroimage*, *44*, 190–199.

Ruff, C. C., Bestmann, S., Blankenburg, F., Bjoertomt, O., Josephs, O., Weiskopf, N., … Driver, J. (2008). Distinct causal influences of parietal versus frontal areas on human visual cortex: evidence from concurrent TMS-fMRI. *Cerebral Cortex (New York, N.Y. : 1991)*, *18*, 817–827.

Saalmann, Y. B., Pigarev, I. N., & Vidyasagar, T. R. (2007). Neural mechanisms of visual attention: how top-down feedback highlights relevant locations. *Science (New York, N.Y.)*, *316*, 1612–1615.

Sauseng, P., Klimesch, W., Stadler, W., Schabus, M., Doppelmayr, M., Hanslmayr, S., … Birbaumer, N. (2005). A shift of visual spatial attention is selectively associated with human EEG alpha activity. *The European Journal of Neuroscience*, *22*, 2917–2926.

Scheeringa, R., Fries, P., Petersson, K. M., Oostenveld, R., Grothe, I., Norris, D. G., … Bastiaansen, M. C. (2011). Neuronal dynamics underlying high- and low-frequency EEG oscillations contribute independently to the human BOLD signal. *Neuron*, *69*, 572–583.

Shulman, G. L., & Corbetta, M. (2012). Two Attentional Networks: Identification and Function within a Larger Cognitive Architecture. In *Cognitive Neuroscience of Attention*, ed. MI Posner, pp. 113–28. New York, NY, USA: The Guilford Press

Siegel, M., Donner, T. H., Oostenveld, R., Fries, P., & Engel, A. K. (2008). Neuronal synchronization along the dorsal visual pathway reflects the focus of spatial attention. *Neuron*, *60*, 709–719.

Sylvester, C. M., Shulman, G. L., Jack, A. I., & Corbetta, M. (2007). Asymmetry of anticipatory activity in visual cortex predicts the locus of attention and perception. *The Journal of Neuroscience : The Official Journal of the Society for Neuroscience*, *27*, 14424–14433.

Taulu, S., & Simola, J. (2006). Spatiotemporal signal space separation method for rejecting nearby interference in MEG measurements. *Physics in Medicine and Biology*, *51*, 1759–1768.

Taulu, S., Simola, J., & Kajola, M. (2005). Applications of the signal space separation method (SSS). *IEEE Trans Signal Process*, *53*, 3359–3372.

Thiel, C. M., Zilles, K., & Fink, G. R. (2004). Cerebral correlates of alerting, orienting and reorienting of visuospatial attention: an event-related fMRI study. *Neuroimage*, *21*, 318–328.

Uusitalo, M. A., & Ilmoniemi, R. J. (1997). Signal-space projection method for separating MEG or EEG into components. *Medical &Amp; Biological Engineering &Amp; Computing*, *35*, 135–140.

Van Veen, B. D., van Drongelen, W., Yuchtman, M., & Suzuki, A. (1997). Localization of brain electrical activity via linearly constrained minimum variance spatial filtering. *IEEE Transactions on Bio-Medical Engineering*, *44*, 867–880.

von Stein, A., & Sarnthein, J. (2000). Different frequencies for different scales of cortical integration: from local gamma to long range alpha/theta synchronization. *Int J Psychophysiol*, *38*, 301–313.

Vossel, S., Geng, J. J., & Fink, G. R. (2014). Dorsal and ventral attention systems: distinct neural circuits but collaborative roles. *The Neuroscientist : a Review Journal Bringing Neurobiology, Neurology and Psychiatry*, *20*, 150–159.

Vossel, S., Thiel, C. M., & Fink, G. R. (2006). Cue validity modulates the neural correlates of covert endogenous orienting of attention in parietal and frontal cortex. *Neuroimage*, *32*, 1257–1264.

Vossel, S., Weidner, R., Driver, J., Friston, K. J., & Fink, G. R. (2012). Deconstructing the architecture of dorsal and ventral attention systems with dynamic causal modeling. *The Journal of Neuroscience : The Official Journal of the Society for Neuroscience*, *32*, 10637–10648.

Vossel, S., Weidner, R., Thiel, C. M., & Fink, G. R. (2009). What is "odd" in Posner's location-cueing paradigm? Neural responses to unexpected location and feature changes compared. *Journal of Cognitive Neuroscience*, *21*, 30–41.

Wilson, T. W., Heinrichs-Graham, E., & Becker, K. M. (2014). Circadian modulation of motor-related beta oscillatory responses. *Neuroimage*, *102*(Pt 2), 531–539.

Wilson, T. W., Heinrichs-Graham, E., Proskovec, A. L., & McDermott, T. J. (2016). Neuroimaging with magnetoencephalography: A dynamic view of brain pathophysiology. *Translational Research : The Journal of Laboratory and Clinical Medicine*, *175*, 17–36.

Wilson, T. W., Heinrichs-Graham, E., Robertson, K. R., Sandkovsky, U., O'Neill, J., Knott, N. L., … Swindells, S. (2013). Functional brain abnormalities during finger-tapping in HIV-infected older adults: a magnetoencephalography study. *J Neuroimmune Pharm*, *8*, 965–974.

Womelsdorf, T., & Fries, P. (2007). The role of neuronal synchronization in selective attention. *Current Opinion in Neurobiology*, *17*, 154–160.

Xuan, B., Mackie, M. A., Spagna, A., Wu, T., Tian, Y., Hof, P. R., & Fan, J. (2016). The activation of interactive attentional networks. *Neuroimage*, *129*, 308–319.

## SUPPORTING INFORMATION

Additional Supporting Information may be found online in the supporting information tab for this article.

**How to cite this article:** Proskovec AL, Heinrichs-Graham E, Wiesman AI, McDermott TJ, Wilson TW. Oscillatory dynamics in the dorsal and ventral attention networks during the reorienting of attention. *Hum Brain Mapp*. 2018;39:2177–2190. https://doi.org/10.1002/hbm.23997